dence on Δ (an upward shift of the oxygen 2p orbitals). It is seen that the HOMO energy becomes almost independent of angle, if it becomes too close to the empty 5f-like levels. (The sum of the five lowest orbital energies is approximately independent of the angle and is therefore omitted from Figures 4 and 5.) The central feature for Th, as a function of decreasing bond length, is seen to be that the "linearizing" influence of MO 10 grows faster than the bending influence of MO 11, with shortening bond length. This tendency is seen quantitatively in Table VIII.

Comparing the two metals, the linearizing tendency of MO 10 and the R dependence of this trend are very similar. The difference appears in MO 11 where the bending tendency is stronger for Th than for U.

A variation of Δ for ThO_2 at 191 pm gives a bent molecule for Δ = 0, two minima (at 180 and 100°) for Δ = 2 and a clearly linear molecule at 4 eV. For uranyl, all Δ values give a linear molecule (see Figure 5).

Without the 6p orbitals, using a 7s7p6d5f metal basis, all cases were linear but only very weakly.

The Walsh-type REX argument, based on the energies of MOs 10 and 11, can be summarized as follows (the bond lengths are here input data).

ThO_2 is bent, first because it has a larger bond length and therefore a weaker "linearizing" tendency from MO 10 (see Figure 4), second because it has lower lying 6d levels (in ref 11 as in Figure 2 but not in Figure 1) that tend to bend the molecule and, third because it has a higher lying 5f level, which therefore does not "flatten" the HOMO, MO 11.

Inversely, uranyl is linear because it has a shorter bond length (due to good multiple bonding, a smaller 6p core and, eventually, its positive net charge) and has therefore a strong linearizing tendency from the MO 10, second uranium has higher lying input 6d levels, and third uranium has lower lying input 5f levels, which tend to "flatten" MO 11.

To obtain the strong 5f character of MO 11 the REX/EHT requires the "pushing from below" by the semicore 6p AOs. With the 6p but without the 5f orbitals, MO 11 would be strongly bending.[4,12] Without the 6p orbitals, MO 10 would not become strongly linearizing because this trend was attributed to 2p–6p repulsion.[14]

As a technical detail, it is interesting that the σ_u MO 11 is apparently repelled by the 5f band above it, although none of the other 5f levels have a σ_u symmetry that could lead to a noncrossing. Similar stationary levels have been reported elsewhere[22-24] for Hamiltonian matrices of the type

$$\mathbf{h} = \begin{pmatrix} \alpha_1 & 0 & a \\ 0 & \alpha_1 & b \\ a & b & \alpha_3 \end{pmatrix} \tag{5}$$

In that case the combination $b|1\rangle - a|2\rangle$ of the two degenerate orbitals is orthogonal to $|3\rangle$ and stays at $E = \alpha_1$.

In the present case, we instead have the matrix structure

$$\mathbf{h} = \begin{pmatrix} \alpha_{6p} & 0 & a \\ 0 & \alpha_{5f} & b \\ a & b & \alpha_{2p} \end{pmatrix} \tag{6}$$

This matrix has an (Newton–Raphson, $\mathbf{S} = \mathbf{1}$, $\alpha_{5f} = 0$) eigenvalue at

$$E \cong \alpha_{6p} b^2/(a^2 + b^2 - \alpha_{6p}\alpha_{2p}) \tag{7}$$

As, typically, $a = +17$ eV, $b = +3$ eV, $\alpha_{6p} = -19$ eV, $\alpha_{2p} = -6$ eV for Δ = 0, this level lies about 1 eV below α_{5f}.

Acknowledgment. We thank Jukka Tulkki for some atomic DF calculations, Evert Jan Baerends and Jaap Snijders for helpful comments, and a reviewer for asking that the last point be clarified.

Registry No. UO_2^{2+}, 16637-16-4; ThO_2, 1314-20-1; $(cp)_4Th$, 1298-75-5; $(cp)_4U$, 1298-76-6; $Th(COT)_2$, 12702-09-9; $U(COT)_2$, 11079-26-8; $Pa(COT)_2$, 51056-18-9; $Np(COT)_2$, 37281-22-4.

(22) Burdett, J. K. *Prog. Solid State Chem.* **1984**, *15*, 173, 241.
(23) Hoffmann, R.; Li, J.; Wheeler, R. A. *J. Am. Chem. Soc.* **1987**, *109*, 6600.
(24) Boerrigter, P. M.; Snijders, J. G.; Dyke, J. M. *J. Electron Spectrosc. Relat. Phenom.* **1988**, *46*, 43.

Contribution from the Department of Chemistry, University of Leuven, Celestijnenlaan 200F, 3030 Heverlee, Belgium

Electronic Configuration and Orbital Energies: The 3d–4s Problem

L. G. Vanquickenborne,* K. Pierloot, and D. Devoghel

Received May 6, 1988

With the use of the numerical Hartree–Fock method, a set of average-of-configuration calculations have been carried out for the atoms from H to Cu, as well as for the corresponding mono- and dipositive ions. The focus of this work is on the study of the occupation of 3d and/or 4s orbitals. Attempts are made to relate configurational energy differences to simple orbital energy differences, so as to provide additional insight into the Aufbau principle of the periodic system of the elements.

I. Introduction

In discussions of the Aufbau principle of the elements, it is customary to start from a qualitative energy diagram,[1-3] where the evolution of the different orbital energies ε is shown as a function of Z. Up to argon, the ground-state configuration of the atoms can be obtained by filling the orbitals in the expected sequence 1s, 2s, 2p, 3s, 3p. The first deviation from the hydrogenic order is apparently due to a crossover of the 3d and 4s curves. Obviously, the 3d–4s crossover has important consequences for the electronic configuration of transition-metal elements.

Yet, it appears that the theoretical basis of the $\epsilon(Z)$ orbital energy diagram is somewhat unclear: the diagrams presented in the literature either are purely qualitative, are deduced from spectral data in a semiempirical way, or else are based on very approximate Thomas–Fermi-type calculations. To our knowledge, no systematic ab initio treatment is available, describing the evolution of the orbital energies ε as a function of Z.

It is the purpose of this paper (i) to discuss a systematic series of ab initio calculations on the relevant configurations with 4s and/or 3d occupation, from H up to Cu, (ii) to relate configurational energy differences to orbital energy differences, and (iii) to extend the calculations to the mono- and dipositive ions of the elements.

II. Hartree–Fock Treatment of the Average of a Configuration

For the systems under consideration, it is possible to predict the experimental ground states and to calculate quantitatively term splittings and ionization energies by MCSCF type techniques and configuration interaction.[4-7] If one is more interested in general

(1) Latter, R. *Phys. Rev.* **1955**, *99*, 510.
(2) Levine, I. N. *Quantum Chemistry*; Allyn & Bacon, Inc.: Boston, MA, 1974; p 244.
(3) Cotton, F. A.; Wilkinson, G. *Advanced Inorganic Chemistry*, 5th ed.; J. Wiley & Sons, Inc.: New York, 1988; p 628.

0020-1669/89/1328-1805$01.50/0

Table I. Energy Difference (in eV) between the Ground Configuration Average and a Number of Excited States and Configuration Averages in Sc, Ti^+, and V^{2+} ($N = 3$)[a]

			ΔE_{exp}	ΔE_{SCF}	ΔE_{frav}
Sc	Avd^1s^2	^2D	0	0	0
	d^2s^1	^4F	1.427	1.007	1.014
		^2F	1.846	1.772	1.890
		^2D	2.097	2.181	2.182
		^4P	2.129	2.063	2.094
		^2G	2.500	2.669	2.686
		^2P	2.555	2.924	2.969
		^2S	3.327	4.438	4.696
	Avd^2s^1		1.992	1.934	1.971
	Avd^3s^0		4.638	5.464	5.477
Ti^+	Avd^2s^1		0	0	0
	Avd^1s^2		2.152	2.763	2.740
V^{2+}	Avd^3s^0		0	0	0
	Avd^2s^1		4.830	4.589	4.590

[a] The experimental energies ΔE_{exp} are taken from Sugar and Corliss;[11] ΔE_{SCF} is the energy difference between the situations under consideration, based on the solution of the Hartree–Fock equations for each state individually; ΔE_{frav} is the energy difference between the situations under consideration, calculated from one set of frozen orbitals per configuration.

qualitative features however, and especially if one is interested in the relationship between orbital energies and state energies, Hartree–Fock calculations are perhaps more appropriate—though certainly less accurate.

For each one of the neutral atoms from H to K, two different configurations are relevant for our purposes: ($...3d^14s^0$) and ($...3d^04s^1$). Both configurations are characterized by $N = 1$, where N is the number of electrons in the 3d,4s orbital subset. For the heavier atoms, from Ca to Cu, where $N \geq 2$, *three* different configurations should be considered: $3d^p4s^q$, where $q = 0$, 1, or 2 and where $p + q = N$. A complete Hartree–Fock treatment of all these systems would be rather involved and probably not very illuminating. Indeed, most of the configurations give rise to several multiplets, and each multiplet is characterized by its own set of orbitals and orbital energies.

Therefore, we prefer to work within the average-of-configuration procedure. That is, we solved the Hartree–Fock equation for the average field of each particular configuration, using Fischer's numerical Hartree–Fock method.[8,9] In this way, we obtain the best possible orbitals describing simultaneously the different states corresponding to any one of the relevant configurations. It is well-known that these average orbitals are only very slightly different from the optimal Hartree–Fock orbitals for each individual state.[10] As a matter of fact, if the average orbitals are frozen and used to calculate the different multiplet energies, only very small errors result. Table I illustrates some of these points for $N = 3$ systems. First of all, it is clear that the experimental energy difference between two configuration averages is only known if *all* states of both configurations have been observed and identified. Even for the first transition series, this condition is only occasionally satisfied. Table I shows the experimental relative energy for the three Sc configuration averages, d^1s^2, d^2s^1, and d^3s^0, and for two of the three Ti^+ and V^{2+} configuration averages (the experimental information is lacking for Ti^+ d^3s^0 and for V^{2+} d^1s^2). Table I also shows the energy of the seven individual states (averaged over J) corresponding to the Sc d^2s^1 configuration. The difference between ΔE_{SCF} and ΔE_{frav} is only of the order of 1%, showing that the loss in numerical accuracy resulting from our procedure is actually quite small.

For the individual states, the agreement between the experimental ΔE_{exp} on the one hand and ΔE_{SCF} or ΔE_{frav} on the other hand is qualitatively satisfactory, but quantitatively the error can amount to more than 40%. In all but one case, the relative sequence of the d^2s^1 states is predicted correctly; the inversion of the (close-lying) ^4P and ^2D states is probably due to the fact that Hartree–Fock calculations tend to favor high-spin states (characterized by a correspondingly high Pauli correlation).

In the averaging process, the differential Pauli correlations tend to cancel; as a consequence, the relative energy of configuration averages is more reliable than the relative energy of the individual states: the error (with respect to experiment) is smaller, and the correct sequence is predicted in all cases.

The main advantages of the average-of-configuration formalism are however that (i) we can now limit ourselves to a comparison of only two or three different situations, each one being the weighted mean of a number of states and (ii) the orbital energies of open and closed shells now *both* satisfy Koopmans' theorem, and therefore they do have a comparable meaning.[9]

The here presented treatment is related to the work of Claydon and Carlson,[12] who discussed the results of restricted Hartree–Fock calculations on the ground states of first-row transition metals. The Claydon–Carlson paper did not focus on orbital energies however, and as such, it left a number of questions unanswered, giving rise to several conflicting discussions on ground-state energies in terms of orbital occupancy.[13-18]

III. Energy Expressions

Quite generally, the total energy of a ($...3d^p4s^q$) configuration average is given by[9]

$$E_{av}(d^ps^q) = E_c + p\omega_{3d} + q\omega_{4s} + \frac{p(p-1)}{2}(3d,3d) + \frac{q(q-1)}{2}(4s,4s) + pq(3d,4s) \quad (1)$$

Here, E_c is the core energy, containing the total one-electron contribution of the core, as well as the total repulsion between these electrons, but *not* the repulsion between the core and the 3d or 4s electrons. For the 3d transition metals, the core corresponds to the argon core; for the $N = 1$ systems, one electron is promoted from the highest occupied orbital of the ground-state configuration to 3d or 4s. Therefore, the number of core electrons decreases with decreasing Z, being equal to the total number of electrons minus one.[19] The parameter ω can be considered as the effective one-electron energy of a valence (i.e. 3d or 4s) electron moving in the average field of the core:

$$\omega_{3d} = t_{3d} + l_{3d} + (c,3d)$$
$$\omega_{4s} = t_{4s} + l_{4s} + (c,4s) \quad (2)$$

t is the kinetic energy, l is the electron–nucleus attraction, (c,3d) and (c,4s) are the average repulsion between one 3d (or 4s)

(4) Bauschlicher, C. W., Jr.; Walch, S. P.; Partridge, H. *J. Chem. Phys.* **1982**, *76*, 1033.
(5) Dunning, T. H.; Botch, B. H.; Harrison, J. F. *J. Chem. Phys.* **1980**, *72*, 3419.
(6) Fischer, C. F. *J. Chem. Phys.* **1982**, *76*, 1934.
(7) Botch, B. H.; Dunning, T. H.; Harrison, J. F. *J. Chem. Phys.* **1981**, *75*, 3466.
(8) Fischer, C. H. *Comput. Phys. Commun.* **1969**, *1*, 151. Fischer, C. H. *The Hartree–Fock Method for Atoms*; Wiley Interscience: New York, 1977.
(9) Slater, J. C. *Quantum Theory of Atomic Structures*; McGraw-Hill: New York, 1960; Vol. II.
(10) Vanquickenborne, L. G.; Haspeslagh, L. *Inorg. Chem.* **1982**, *21*, 2448.
(11) Sugar, J.; Corliss, C. J. *J. Phys. Chem. Ref. Data* **1978**, *7*, 1191; **1979**, *8*, 1; **1980**, *9*, 473.
(12) Claydon, C. R.; Carlson, K. D. *J. Chem. Phys.* **1968**, *49*, 1331.
(13) Hochstrasser, R. M. *J. Chem. Educ.* **1965**, *42*, 154.
(14) Pilar, F. L. *J. Chem. Educ.* **1978**, *55*, 3.
(15) Carlton, T. S. *J. Chem. Educ.* **1979**, *56*, 767.
(16) Pilar, F. L. *J. Chem. Educ.* **1979**, *56*, 767.
(17) De Kock, R. L.; Gray, H. B. *Chemical Structure and Bonding*; Benjamin: New York, 1980.
(18) Cook, D. B. *Mol. Phys.* **1984**, *53*, 631.

(19) In eq 1, we use the designation "valence orbital" for the 3d,4s set and "core orbital" for all lower lying orbitals. This is in line with the conventional terminology for transition metals, but not for the pretransition elements. For instance, for C $1s^22s^22p^13d^1$, we consider $1s^22s^22p^1$ to be the "core" and $3d^1$ to be the "valence" shell. This rather unusual convention allows us to write a single energy expression (eq 1) for all elements under consideration.
(20) Virtual orbital energies cannot be obtained from eq 9, which presuppose occupied orbitals.

electron and the core. If the individual core orbitals are designated as γ

$$(c,3d) = \sum_{\gamma} N_{\gamma}(\gamma,3d)$$
$$(c,4s) = \sum_{\gamma} N_{\gamma}(\gamma,4s) \quad (3)$$

where for instance $(\gamma,3d)$ is the average repulsion between an electron in a γ-core orbital and another one in 3d; N_γ is the number of electrons in γ. In eq 1, (3d,3d) represents the average repulsion between two electrons in the d shell:

$$(3d,3d) = {}^1/_{45}\sum_{a}^{5}\sum_{b}^{5}(2J_{ab} - K_{ab}) \quad (4a)$$

where a and b range over the five 3d orbitals. The corresponding expression for (4s,4s) consists of only one term

$$(4s,4s) = J_{4s,4s} \quad (4b)$$

whereas

$$(3d,4s) = {}^1/_{10}\sum_{a}^{5}(2J_{4s,a} - K_{4s,a}) \quad (4c)$$

All J and K integrals can of course be expressed in terms of the appropriate Slater–Condon parameters G^k and F^k. It is convenient to introduce a separate symbol for the valence-shell repulsion terms in eq 1:

$$C_v = \frac{p(p-1)}{2}(3d,3d) + \frac{q(q-1)}{2}(4s,4s) + pq(3d,4s) \quad (5)$$

Similarly the repulsion between valence shells and core shells can be denoted as

$$C_{cv} = p(c,3d) + q(c,4s) \quad (6)$$

and the total repulsion C becomes

$$C = C_v + C_{cv} + C_c \quad (7)$$

where C_c is the intracore repulsion included in E_c.

The orbital energies ϵ_{3d} and ϵ_{4d} in $3d^p4s^q$ can easily be found from eq 1, since Koopmans' theorem is always satisfied for configuration averages. For instance, from

$$\epsilon_{3d} = E_{av}(d^p s^q) - E_{av}^{p,q}(d^{p-1}s^q) \quad (8)$$

where the superscript p,q means that the frozen orbitals of $d^p s^q$ have to be used, we find

$$\epsilon_{3d} = \omega_{3d} + (p-1)(3d,3d) + q(3d,4s) \quad (9a)$$

and similarly

$$\epsilon_{4s} = \omega_{4s} + (q-1)(4s,4s) + p(3d,4s) \quad (9b)$$

Both ϵ_{3d} and ϵ_{4s} are seen to have their usual meaning as the energy of an electron in a particular orbital, moving in the field of all other electrons.

Substitution of eq 9a,b into eq 1 (and using the definition of C_v, eq 5) gives the total energy in terms of the valence-orbital energies:

$$E_{av}(d^p s^q) = E_c + p\epsilon_{3d} + q\epsilon_{4s} - C_v \quad (10)$$

IV. The $N = 1$ Case

Many of the expressions of the previous section become of course much simpler in the $N = 1$ case. More specifically, when applied to the two configurations $3d^14s^0$ and $3d^04s^1$, eq 9a and 9b become

$$\epsilon_{3d}(d^1s^0) = \omega_{3d}(d^1s^0)$$
$$\epsilon_{4s}(d^0s^1) = \omega_{4s}(d^0s^1) \quad (11)$$

and eq 1 yields

$$E_{av}(d^1s^0) = E_c(d^1s^0) + \omega_{3d}(d^1s^0)$$
$$E_{av}(d^0s^1) = E_c(d^0s^1) + \omega_{4s}(d^0s^1) \quad (12)$$

Table II. Numerical Hartree–Fock Results for the Total Energy (in Atomic Units), Energy Difference (in eV), Orbital Energies (in eV), and Orbital Parameters (in Atomic Units of Length) of Three 19-Electron Systems ($N = 1$): K, Ca^+, and Sc^{2+}

	K	Ca^+	Sc^{2+}
$E_{av}(d^0s^1)$	−599.1650	−676.5702	−758.9811
$E_{av}(d^1s^0)$	−599.0759	−676.4987	−759.0926
$\Delta E_{av}(s \rightarrow d)$	2.424	1.946	−3.034
$\epsilon_{4s}(d^0s^1) = \epsilon_{4s,i}$	−4.013	−11.328	−20.867
$\epsilon_{3d}(d^1s^0) = \epsilon_{3d,f}$	−1.581	−9.717	−24.611
$\epsilon_{3d,f} - \epsilon_{4s,i}$	2.432	1.611	−3.744
r_{4s}	5.2437	3.7284	3.0330
r_{3d}	9.5382	2.3417	1.5436
ΔE_c	−0.008	0.335	0.710

The corresponding energy difference $\Delta E_{av}(s \rightarrow d)$ can therefore be expressed as

$$\begin{aligned}\Delta E_{av}(s \rightarrow d) &= E_{av}(d^1s^0) - E_{av}(d^0s^1) \\ &= E_c(d^1s^0) - E_c(d^0s^1) + \omega_{3d}(d^1s^0) - \omega_{4s}(d^0s^1) \\ &= \epsilon_{3d}(d^1s^0) - \epsilon_{4s}(d^0s^1) + \Delta E_c\end{aligned} \quad (13)$$

where ΔE_c is the relaxation energy of the nontransferred core electrons, due to their shape change following the $4s \rightarrow 3d$ transfer.

Now, the single valence electron moves in a region of space that is well separated from the space occupied by any of the other electrons. As an example, Table II shows a number of illustrative data for the isoelectronic series K, Ca^+, and Sc^{2+}. For the neutral K atom for example, the core electrons are on the average only some 1.5 au or less from the nucleus, whereas $r_{4s} = 5.24$ and $r_{3d} = 9.54$ au (Table II). As a consequence, the core electrons are not very much affected by the presence of the valence electron, and Table II shows that ΔE_c is negligibly small for K, and a fortiori so for the lighter atoms.[21] As a result, for the neutral atoms, the configurational energy difference $\Delta E_{av}(s \rightarrow d)$ can to a good approximation be written as a simple orbital energy difference:

$$\Delta E_{av}(s \rightarrow d) \simeq \epsilon_{3d}(d^1s^0) - \epsilon_{4s}(d^0s^1) = \epsilon_{3d,f} - \epsilon_{4s,i} \quad (14)$$

As stressed before, the two orbital energies refer to *different* configurations (added in parentheses); they are eigenfunctions of *different* Hartree–Fock Hamiltonians. For the here considered $s \rightarrow d$ transition, d^0s^1 is the initial configuration and d^1s^0 the final configuration—hence the shorthand notation in terms of $\epsilon_{3d,f}$ and $\epsilon_{4s,i}$.[23]

Figure 1A shows the evolution of the two orbital energies as a function of Z for the neutral atoms. It is well-known from spectroscopic data[24] on ΔE_{av} that the here presented orbital energy differences reproduce the experimental energy level evolution. Figure 1A confirms the conventional picture of an almost nonpenetrating 3d orbital of nearly constant energy, characterized by $Z_{eff} \simeq 1$ up to K. Due to its nodal structure, the 4s orbital does penetrate the core however. The corresponding decrease in

(21) Following Koopmans' theorem, the value of ΔE_c can formally be subdivided into two components:

$$\Delta E_c = \Delta E_c(d^1) - \Delta E_c(s^1)$$

where $\Delta E_c(d^1)$ and $\Delta E_c(s^1)$ stand for the *positive* relaxation energy accompanying the ionization of the 3d or 4s electron, respectively. The sign of ΔE_c then reflects whether the core electrons are more affected by the presence of the 3d ($\Delta E_c > 0$) or 4s electron ($\Delta E_c < 0$). For K, ΔE_c has a very small negative value, indicating that the valence electron affects the core more when it is in 4s than when it is in 3d ($r_{4s} \ll r_{3d}$)—although the effect is small in both cases. For the positive ions, 3d has contracted much more than 4s, and its interaction with the core has increased significantly; therefore ΔE_c has become positive. A rather detailed analysis of ΔE_c is also given by Calabro and Lichtenberger in ref 22. However, for the K atom, these authors present erroneous relative values of $\Delta E_c(d^1)$ and $\Delta E_c(s^1)$. In ref 14, Pilar claims incorrectly that $\epsilon_{4s} > \epsilon_{3d}$ for both K and Na.

(22) Calabro, D. C.; Lichtenberger, D. L. *Inorg. Chem.* **1980**, *19*, 1732.

(23) The alternative energies $\epsilon_{3d,i}$ and $\epsilon_{4s,f}$ would correspond to virtual orbitals and cannot be given a physical meaning in the same sense as the occupied orbitals.

(24) Moore, C. E. *Atomic Energy Levels as Derived from the Analysis of Optical Spectra*; NBS Circular 467; National Bureau of Standards: Washington, DC, 1952; Vol. II.

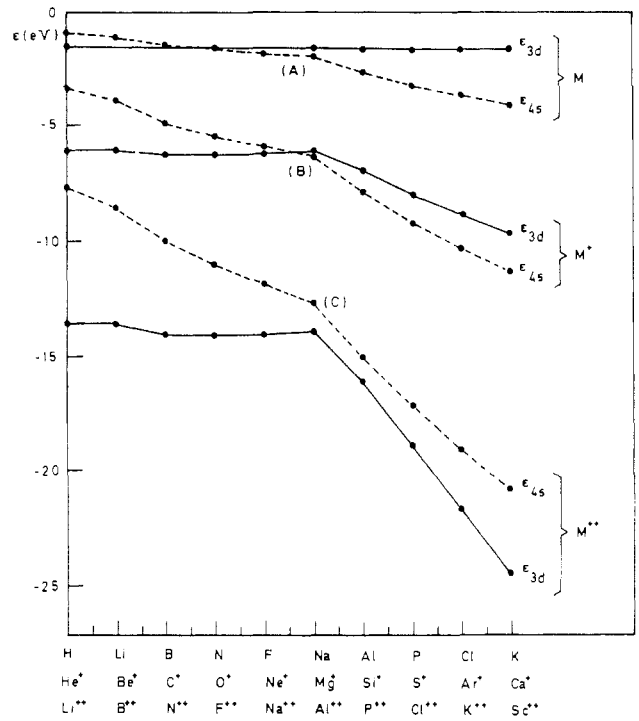

Figure 1. 3d (—) and 4s (- - -) orbital energies calculated in the $(3d)^1$ and $(4s)^1$ configurations as a function of Z ($N = 1$ in all cases) for the neutral atoms (M) and the mono- (M^+) and dipositive (M^{2+}) ions preceding the transition metals in the periodic system. Isoelectronic series are represented on a vertical line. In the terminology of an s → d transition, $\epsilon_{3d} = \epsilon_{3d,f}$ and $\epsilon_{4s} = \epsilon_{4s,i}$. According to eq 14 the difference $(\epsilon_{3d,f} - \epsilon_{4s,i})$ also represents the energy change involved in the $s^1 \rightarrow d^1$ transition.

energy leads to the well-known crossover in the neighborhood of C (in perfect agreement with experiment) and a positive $(\epsilon_{3d,f} - \epsilon_{4s,i})$ value of up to 2.4 eV for K (as defined in eq 14).

It is important to realize however that the general features of the $\epsilon(Z)$ curves as shown in Figure 1 are strongly charge dependent. Parts B and C of Figure 1 show how the situation is changed from neutral M to M^+ and M^{2+}. Increasing the nuclear charge (at constant N) stabilizes all orbitals, but especially 3d. This is already evident in the one-electron case, where the stabilization of 3d with respect to 4s increases as $Z^2(^1/_9 - ^1/_{16})$. As a consequence of the corresponding orbital contraction (see Table II), the 3d orbital does overlap with the 3s and 3p orbitals in the ions M^+ and M^{2+}, so that if we start from the point where these core orbitals are filled, the effective charge felt by the 3d electron increases abruptly, and ϵ_{3d} drops rather steeply.[25] The 4s orbital is much less affected by the Z increase. As a result, the 3d,4s crossover comes later for M^+ and is inexistent for M^{2+}.

As can be seen from Table II, the 3d contraction also affects the value of ΔE_c, which is no longer negligible (see eq 13). Still, ΔE_c decreases to the left side of Figure 1, and the values of Table II are larger than those of any of the preceding elements. Therefore, eq 14 remains a valid description, and even for the positive ions, it remains qualitatively correct to approximate ΔE_{av}(s → d) by the orbital energy difference $\epsilon_{3d,f} - \epsilon_{4s,i}$.

The curves of Figure 1 have been discontinued when the argon core is fully occupied, because at that point further addition of electrons makes $N \geq 2$, so that we have to consider *three* instead of only two configurations, with $q = 0$, 1, or 2 in $3d^p4s^q$. In the $3d^p4s^q$ configurations, neither of the valence orbitals is in general virtual; each one of the three relevant Hartree–Fock Hamiltonians yields one or two (occupied) orbital energies leading to a total of four or five ϵ values for each atom or ion. In the next section, we describe in detail the results for $2 \leq N \leq 10$.

(25) It is interesting to observe that ϵ_{3d} remains virtually constant (both for M^+ and M^{2+}), corresponding to $Z \simeq 2$ and $Z \simeq 3$, respectively, as long as 3s remains unoccupied. This suggests that 3d does penetrate 3s and 3p, but not the inner core $1s^22s^22p^6$—at least not to a significant extent.

V. Results for $N > 1$

1. Total Energies. Figure 2A shows the total energy evolution of the three configuration averages for the neutral metal atoms M and for the mono- and dipositive ions M^+, M^{2+}. The energy is plotted not as a function of Z but as a function of N, the number of valence (3d and/or 4s) electrons, where $N \geq 2$. As a consequence, isoelectronic series (such as Sc, Ti^+, V^{2+} or Co, Ni^+, Cu^{2+}) are represented on the same vertical line.[26] For $N = 3$, Figure 2A incorporates the results of Table I.

The neutral atoms (except for the heaviest: Ni and Cu) have a d^ns^2 ground configuration, and their energy increases with each s → d transition:

$$\text{light M:}\quad E_{av}(d^ns^2) < E_{av}(d^{n+1}s^1) < E_{av}(d^{n+2}s^0) \quad (15a)$$

For the M^{2+} ions one has exactly the opposite situation:

$$\text{all } M^{2+}\text{:}\quad E_{av}(d^{n+2}s^0) < E_{av}(d^{n+1}s^1) < E_{av}(d^ns^2) \quad (15b)$$

The monopositive ions M^+ have an intermediate position: for $N \geq 6$ they follow the same pattern as the dipositive ions (15b), whereas for $N < 6$ they are closer to the neutral heavy atoms (Ni, Cu) with a $3d^{n+1}4s^1$ ground configuration.

In summary, Figure 2A shows quite clearly how the tendency to populate 3d increases with the number of valence electrons and with the charge of the ion. Indeed, for a given degree of ionization, the curves of Figure 2A illustrate how the relative stabilities of $3d^{n+2}4s^0$ and $3d^{n+1}4s^1$ increase with respect to that of $3d^n4s^2$, when the number of valence electrons increases: all curves of Figure 2A have negative slopes at all points. Also, ionization is seen to have a very drastic effect on the relative stability of the three configurations: the more positive the ion, the more the s^2 population becomes unstable.[27]

It is also interesting to observe that, for a given number of valence electrons N and a given nuclear charge Z, the first s → d transition ($d^ns^2 \rightarrow d^{n+1}s^1$) is always more favorable, in that either it requires less energy or else it releases more energy than the second one ($d^{n+1}s^1 \rightarrow d^{n+2}s^0$).

$$\Delta E_{av}(d^ns^2 \rightarrow d^{n+1}s^1) < \Delta E_{av}(d^{n+1}s^1 \rightarrow d^{n+2}s^0) \quad (16)$$

2. Orbital Energies of 3d and 4s. The orbital energies of 3d and 4s, corresponding to the different configurations of M, M^+, and M^{2+} are shown in Figure 3. As before, virtual orbitals are not included, because they do not have the same physical meaning as the occupied orbitals.

The most striking feature of Figure 3 is of course the expected appearance of five orbital energies (for each entity M, M^+, and M^{2+}) rather than just two as in Figure 1. In order to link the two figures, the 4s curve of $3d^{n+1}4s^1$ and the 3d curve of $3d^{n+2}4s^0$ could be extrapolated to $N = 1$ (or $n = -1$); this extrapolation yields two points, which are exactly coincident with the rightmost points of Figure 1. The appearance of the three additional curves in Figure 3 is the most obvious manifestation of the inadequacy of the conventional $\epsilon(Z)$ curves commonly used in discussions of the Aufbau principle.[1-3] Apparently, the energies of the 3d and the 4s orbitals increase (at fixed Z and N) with increasing 3d population—and much more so for 3d than for 4s. Before we carry out a more detailed analysis of this phenomenon, it is interesting to highlight some of the other qualitative features of Figure 3.

As could be expected, the slope of all orbital energy curves is negative. Indeed, going from one point on such a curve to the next one corresponds to increasing Z by 1 unit, while at the same time adding one d electron. As a consequence of this operation, both orbitals are stabilized, but 3d more so than 4s. This evolution can be compared with the application of Slater's screening rules,[28,29] where the addition of one d electron and 1 unit of nuclear

(26) Strictly speaking, we should use a different symbol for E_{av} in eq 1 and E_{av} in Figure 2 (where relative quantities are shown, as detailed in the figure caption). However, no confusion is possible and the meaning of the symbols is always obvious from the context; in order to alleviate the notation, we will use the same symbol in both cases.

(27) Figure 2 does not contain any information on ionization energies, since the reference situation for each ion separately has been set equal to zero.

(28) Slater, J. C. *Phys. Rev.* **1930**, *36*, 57.

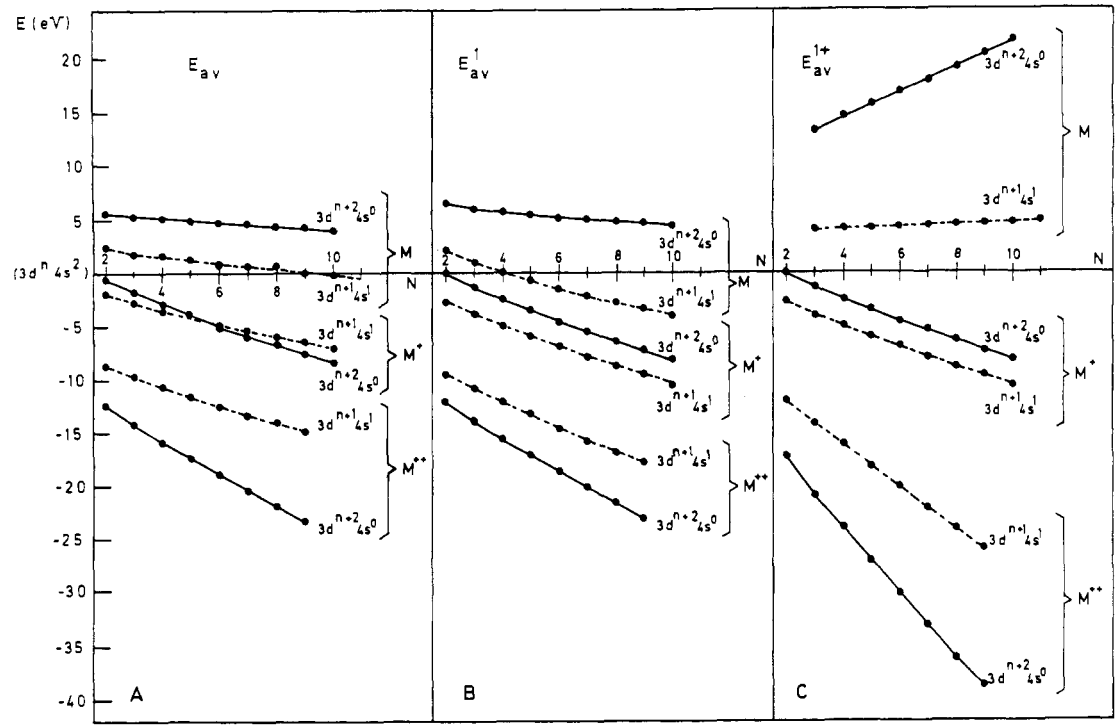

Figure 2. (A) Total average energy E_{av} (in eV) of the first-row transition metals M and their ions M^+ and M^{2+} as a function of the number of valence (3d and/or 4s) electrons N. The energy is given for the $3d^{n+2}4s^0$ (—) and $3d^{n+1}4s^1$ (---) configuration averages, in each case with respect to $3d^n4s^2$ ($N = n + 2$). The abscissa thus corresponds to a superposition of three situations: for any given value of N, it represents the neutral atom, the monopositive ion, and the dipositive ion in the $3d^n4s^2$ configuration (e.g. Sc, Ti^+, and V^{2+} in $3d^14s^2$ are superposed at $N = 3$ and $E_{av} = 0$). All the results were obtained from numerical Hartree–Fock calculations. (B) Total average energy $E_{av}{}^1$ (in eV) of the first-row transition metals M and their ions M^+ and M^{2+} as a function of N. The $E_{av}{}^1$ energies were calculated on the basis of the frozen orbitals of the $3d^{n+1}4s^1$ configuration for each ion. (C) Total average energy $E_{av}{}^{1+}$ (in eV) of the first-row transition metals M and their ions M^+ and M^{2+} as a function of N. The $E_{av}{}^{1+}$ energies were calculated on the basis of the frozen orbitals of the $3d^{n+1}4s^1$ of the M^+ ion; therefore, the M^+ curves in (B) and (C) are identical.

charge is predicted to induce a decrease in the effective nuclear charge Z_{eff} by $1 - 0.35 = 0.65$ units for 3d, but only $1 - 0.85 = 0.15$ units for 4s. Apparently, Slater orbitals are roughly similar to the SCF orbitals, where the same evolution is found; therefore $\epsilon_{4s} - \epsilon_{3d}$ increases with N.

A comparison of the three parts of Figure 3 shows that, for constant N, progressive ionization also pulls the two orbitals strongly apart. Indeed, for any specific choice of configuration, ionization is seen to stabilize both orbitals very strongly, but 3d always drops more in energy than 4s. Again, this evolution may be compared with Slater-type orbitals, where $Z \rightarrow Z + 1$ (for constant N) induces $Z_{eff} \rightarrow Z_{eff} + 1$ in both cases, but where the orbital exponent is $Z_{eff}/3$ for 3d and only $Z_{eff}/3.7$ for 4s. Therefore, $\epsilon_{4s} - \epsilon_{3d}$ increases upon increasing the positive charge on the metal (other things being kept equal).

The general trends of Figure 3 thus confirm the preliminary conclusions from Figure 2A: the stability of the 3d orbital—with respect to the 4s orbital—increases in the same circumstances that make configurations with increasing d population comparatively more stable. The two extreme cases are Cu^{2+} on the one side, where 3d is some 30 eV below 4s, and neutral Ca on the other side, which is the only case in Figure 3 where 3d is actually above 4s.

Apart from Ca, and more specifically, *for all transition metals*—neutral or positively charged—*in any given particular configuration*

$$\epsilon_{3d}(d^p s^q) - \epsilon_{4s}(d^p s^q) < 0 \qquad (17a)$$

Therefore, a very simple ab initio answer is available in the controversy[13-18] on the orbital energies: for transition metals and their ions (but not for Ca), 4s is always above 3d. This means that the hydrogenic sequence has been restored at, or just before, Sc.

It is instructive to compare the evolution of the orbital energy (as displayed in Figure 3) with the corresponding evolution in orbital size. Figure 4 shows the expectation value of r_{3d} and r_{4s} as a function of N, for those configurations where both orbitals are occupied simultaneously[30] ($d^n s^2$ and $d^{n+1}s^1$). Figure 4 shows that a 3d electron is on the average much closer to the nucleus than a 4s electron, irrespective of charge and configuration. Table III confirms this picture by detailing the different energy components of 3d and 4s for the example of $N = 3$, that is the isoelectronic series Sc, Ti^+, V^{2+}. The smaller size of 3d finds expression in a correspondingly larger electron–nucleus attraction, a larger electron–core repulsion, and a higher kinetic energy than those of 4s. The diffuseness of 4s is also apparent from the valence repulsion parameters in Table III. In any given column, we find

$$(4s,4s) < (3d,4s) < (3d,3d) \qquad (18)$$

suggesting that the average distance between two electrons in a 4s orbital is quite large, even larger than that between one electron in a 4s orbital and another one in 3d. From eq 18 and 9, it is clear that the 4s orbital must carry less valence repulsion than the 3d orbital. Still, the dominant contributions in the orbital energy, determining the relative order of ϵ_{3d} and ϵ_{4s}, are the one-electron energies ω—more specifically, the nuclear attraction terms I. The dominance of the one-electron contributions ω may be at the basis of the simple rationalization of Figure 3 in terms of Slater-type orbitals and effective nuclear charges.

3. Orbital Energy and Relaxation Phenomena. The fact that eq 17 holds even for those atoms where Figure 2 shows $d^n s^2$ or $d^{n+1}s^1$ to be the lowest configuration clearly illustrates that eq 17

(29) According to Slater's theory the total energy of an atom or ion is given by (in Ha): $E = \sum_i -{}^1/_2(Z_{eff,i}/n_i^*)^2$ where i runs over all electrons, $n_i^* = n_i = 3$ for 3d, and $n_i^* = 3.7$ for 4s. Although the individual $\epsilon_i \neq -{}^1/_2(Z_{eff,i}/n_i^*)^2$, the general trends of the ϵ_i evolution can be expected to be described approximately by the evolution of $-(Z_{eff,i}/n_i^*)^2$.

(30) An extrapolation of Figure 4 to the $N = 1$ case is possible but should be carried out in the same way that Figures 1 and 3 were linked (section V.2). Therefore, the r_{3d} value of e.g. K $3d^14s^0$ (Table II) *cannot* be seen as an extension of any of the two M curves in Figure 4, since the latter correspond to $3d^n4s^2$ and $3d^{n+1}4s^1$, but not to $3d^{n+2}4s^0$.

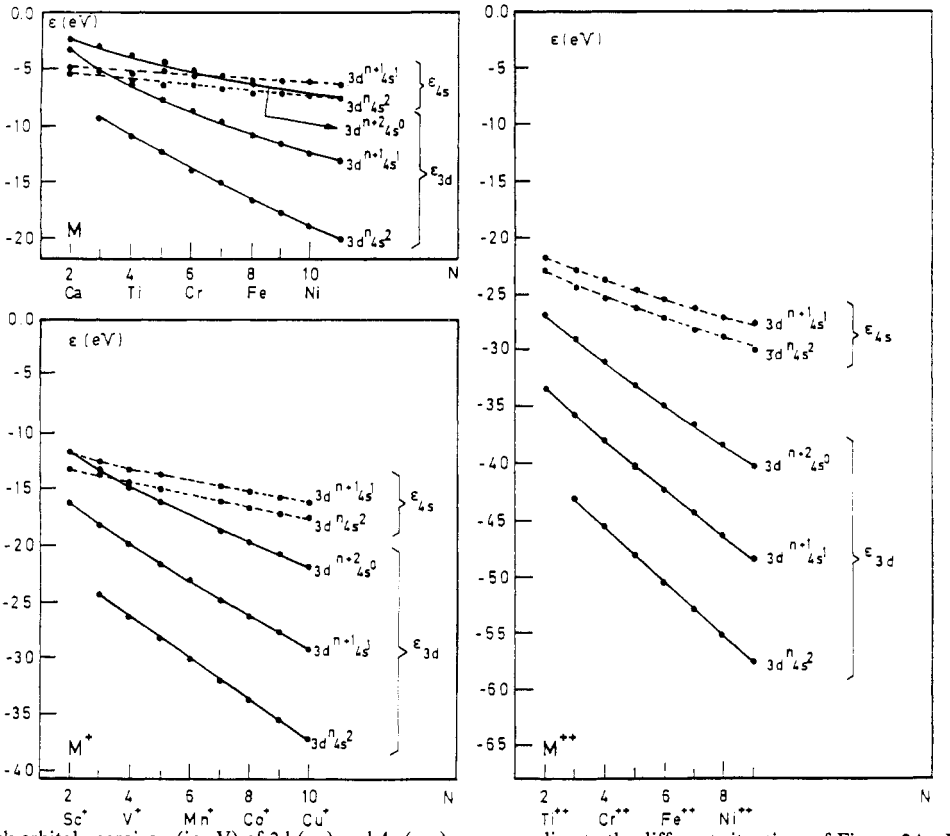

Figure 3. Hartree–Fock orbital energies ϵ (in eV) of 3d (—) and 4s (- - -) corresponding to the different situations of Figure 2A. For the configuration $d^{n+2}s^0$, no ϵ_{4s} curve is included (virtual orbitals were not considered). N is the number of valence electrons (3d and/or 4s).

Table III. Orbital Energies and Energy Components (in eV), and Orbital Radii (in Atomic Units) for 3d and 4s in the Configurations $3d^14s^2$, $3d^24s^1$, and $3d^3$ of the Isoelectronic Series Sc, Ti^+, V^{2+} ($N = 3$)[a]

	Sc			Ti^+			V^{2+}		
	$3d^14s^2$	$3d^24s^1$	$3d^34s^0$	$3d^14s^2$	$3d^24s^1$	$3d^34s^0$	$3d^14s^2$	$3d^24s^1$	$3d^34s^0$
I_{3d}	−456.577	−390.604	−322.606	−590.568	−545.065	−494.203	−714.563	−675.353	−633.446
t_{3d}	83.682	64.310	47.354	124.122	107.583	90.874	164.303	148.180	132.117
I_{4s}	−183.047	−166.464		−244.810	−226.447		−306.105	−288.504	
t_{4s}	15.236	11.786		27.734	22.752		42.345	36.736	
(c,3d)	348.227	302.148	253.172	422.815	393.328	360.001	484.297	460.215	434.380
(c,4s)	148.218	135.938		185.629	173.087		218.681	207.385	
ω_{3d}	−24.668	−24.145	−22.080	−43.632	−44.154	−43.327	−65.962	−66.958	−66.950
ω_{4s}	−19.593	−18.741		−31.446	−30.608		−45.079	−44.383	
(3d,3d)	(14.746)	12.079	9.404	(18.725)	16.967	14.994	(21.974)	20.531	18.980
(4s,4s)	6.215	(5.698)		7.856	(7.331)		9.274	(8.803)	
(3d,4s)	7.657	6.841		9.671	8.953		11.424	10.787	
ϵ_{3d}	−9.353	−5.227	−3.274	−24.289	−18.229	−13.345	−43.112	−35.637	−28.992
ϵ_{4s}	−5.717	−5.059		−13.919	−12.700		−24.382	−22.806	
r_{3d}	1.6755	2.0942	2.7751	1.3024	1.4485	1.6590	1.1039	1.1863	1.2906
r_{4s}	3.9597	4.3204		3.1231	3.3466		2.6406	2.7831	

[a] The symbols are defined in eq 1–4 and eq 9. All these results were obtained from numerical Hartree–Fock calculations. Values in parentheses are not components of the orbital energy ϵ, but they can be calculated from the orbital functions.

is not be itself conclusive in determining the relative energy of the different configurations. It suggests that $\epsilon_{3d}(d^ps^q) - \epsilon_{4s}(d^ps^q)$ needs to attain a certain (negative) threshold value before the population of 3d becomes energetically favorable.

The existence of this threshold value can be understood by realizing that $\epsilon_{3d}(d^ps^q) - \epsilon_{4s}(d^ps^q)$ may not be the most relevant quantity in discussing $\Delta E_{av}(s \rightarrow d)$. Indeed, already for $N = 1$ systems, it was shown in eq 14 that the most important orbital energy difference was $\epsilon_{3d,f} - \epsilon_{4s,i}$. By way of contrast, eq 17a should be rewritten as

$$\epsilon_{3d,i} - \epsilon_{4s,i} < 0 \qquad (17b)$$

where both orbital energies refer to the *same* (initial) configuration.

Applying now our ($N = 1$) line of thinking to transition metals, we rather should consider

$$\epsilon_{3d,f} - \epsilon_{4s,i} = \epsilon_{3d}(d^{p+1}s^{q-1}) - \epsilon_{4s}(d^ps^q)$$

Now, Figure 3 shows that ϵ_{3d} is an increasing function of 3d population, and therefore $\epsilon_{3d,f} > \epsilon_{3d,i}$. Hence, the existence of a threshold value connected with eq 17 may be related to the fact that the condition $\epsilon_{3d,f} - \epsilon_{4s,i} = 0$ provides a better indication for a change in ground-state configuration than $\epsilon_{3d,i} - \epsilon_{4s,i} = 0$. Therefore, it is important to see how and why ϵ_{3d} changes in an $s \rightarrow d$ transition.

If we compare the different configurations at constant N and Z, Figure 4 and Table III show that both 4s and 3d are characterized by a significant expansion with increasing d population

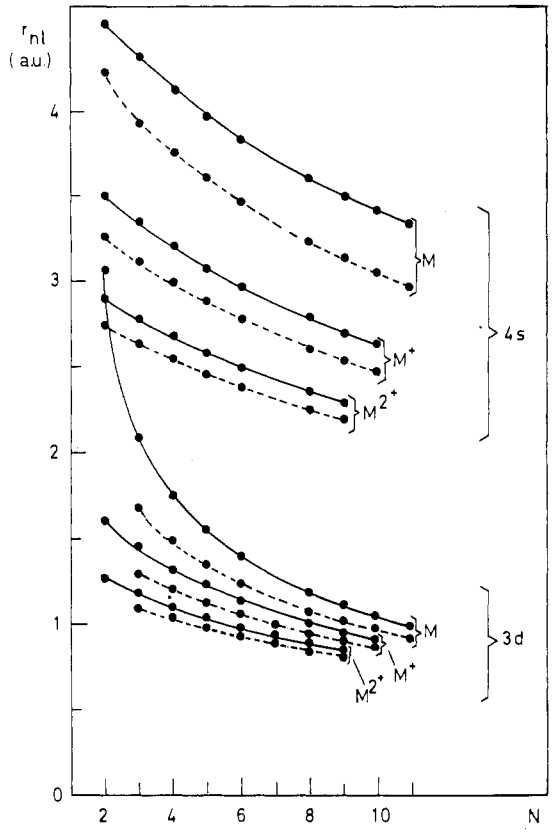

Figure 4. Orbital radii (in atomic units) for 3d and 4s as a function of the number of valence electrons N, corresponding to Figure 2A ($r_{3d} = \langle R_{3d}(r)|r|R_{3d}(r)\rangle$ and $r_{4s} = \langle R_{4s}(r)|r|R_{4s}(r)\rangle$. The results (based on numerical Hartree–Fock calculations) are shown for M, M^+, and M^{2+}, in each case for $3d^{n+1}4s^1$ (—) and $3d^n4s^2$ (---). For $N = 3$, the plot corresponds to the results of Table III.

(relaxation effect), while Figure 3 shows a concomitant upward shift of the orbital energies ϵ_{4s} and ϵ_{3d}. However, the energy increase of both orbitals is *not* a consequence of their expansion, but rather it takes place *in spite of* their expansion. Indeed, the orbital energies ϵ_{4s} and ϵ_{3d} both change as a consequence of the 4s → 3d transition, *even in the absence of relaxation effects*. This can easily be verified by first defining one set of common frozen orbitals for the three configurations, corresponding to a given N and Z, and afterward considering the effect of relaxation. For this purpose, it is natural to start from the orbitals of the intermediate configuration $3d^{n+1}4s^1$; the corresponding parameters will henceforth be designated as

$$\omega_{3d}{}^1,\ \omega_{4s}{}^1,\ (3d,3d)^1,\ (4s,4s)^1,\ (3d,4s)^1 \qquad (19)$$

where the superscript 1 refers to the $4s^1(3d^{n+1})$ population, on which the orbitals are based. If we use eq 9, the orbital energies can now be expressed for any one of the three configurations in terms of the frozen-orbital parameters of eq 19:

$$\epsilon_{3d}{}^1(d^ns^2) = \omega_{3d}{}^1 + (n-1)(3d,3d)^1 + 2(3d,4s)^1$$

$$\epsilon_{3d}{}^1(d^{n+1}s^1) = \omega_{3d}{}^1 + n(3d,3d)^1 + (3d,4s)^1 = \epsilon_{3d}(d^{n+1}s^1)$$

$$\epsilon_{3d}{}^1(d^{n+2}s^0) = \omega_{3d}{}^1 + (n+1)(3d,3d)^1 \qquad (20)$$

Therefore, within the frozen-orbital approximation, each 4s → 3d transition increases the 3d-orbital energy $\epsilon_{3d}{}^1$ by the amount of

$$(3d,3d)^1 - (3d,4s)^1 \qquad (21a)$$

Similarly, the 4s → 3d transition ($d^ns^2 \rightarrow d^{n+1}s^1$) increases $\epsilon_{4s}{}^1$ by

$$(3d,4s)^1 - (4s,4s)^1 \qquad (21b)$$

Because of eq 18, both quantities in eq 21a and 21b are positive. Table III also shows that the numerical values calculated from eq 21a are larger than those calculated from eq 21b.

$$(3d,3d)^1 - (3d,4s)^1 > (3d,4s)^1 - (4s,4s)^1 \qquad (22)$$

As a consequence, the frozen-orbital approximation predicts a pronounced upward shift of the 3d orbital and a smaller upward shift of the 4s orbital, when the 3d population is increased.

Figure 3 shows that this conclusion remains valid for relaxed orbitals, even though relaxation tends to counteract the effect of eq 21. The counteracting effect of relaxation can easily be understood by realizing that a $d^{n+1}s^1 \rightarrow d^{n+2}$ frozen-orbital transition leads to an increase of the valence repulsion felt by the 3d electrons (eq 21a). Therefore, the original 3d orbitals—that were ideally suited to describe the $d^{n+1}s^1$ configuration—will not satisfy the Hartree–Fock equations for the d^{n+2} configurations. In order to reduce the undue repulsion imposed upon them, they will expand, thereby decreasing the absolute value of all the energy contributions in the $d^{n+1}s^1$ columns of Table III. This expansion is then accompanied by a decrease of the 3d-orbital energy: $\epsilon_{3d}(d^{n+2}) < \epsilon_{3d}{}^1(d^{n+2})$. The latter inequality can readily be verified from Table III, where all the relevant numeric parameters are available for $N = 3$. In the opposite case, the $d^{n+1}s^1 \rightarrow d^ns^2$ transition causes a decrease of the valence repulsion of both the 4s and 3d orbitals, inducing now a contraction and a corresponding *increase* of the energy of both orbitals: $\epsilon_{3d}(d^ns^2) > \epsilon_{3d}{}^1(d^ns^2)$ and $\epsilon_{4s}(d^ns^2) > \epsilon_{4s}{}^1(d^ns^2)$.

VI. Analysis of the 4s → 3d Transitions in a Frozen-Orbital Approximation.

With the use of the same set of frozen orbitals as in section V, it is now also possible to calculate the total energy of the three relevant configurations. The result is shown in Figure 2B, which has been set up in exactly the same way as Figure 2A. The general features of both figures are quite similar, and the relative energy of the three considered configurations is generally well predicted by Figure 2B. Both parts A and B of Figure 2 agree in that the neutral atoms with small N are characterized by the energy sequence described by eq 15a, whereas the situation gradually evolves until for dipositive ions the opposite sequence of eq 15b is obtained. However, the d^ns^2–$d^{n+1}s^1$ crossover comes too early for the neutral atoms, and there is no crossover at all for the monopositive ions. Both anomalies are related to the fact that in Figure 2B the first 4s → 3d transition is too low (with respect to Figure 2A), whereas the second 4s → 3d transition is too high. This trend can be traced back to the obvious relationships

$$E_{av}{}^1(d^ns^2) > E_{av}(d^ns^2)$$

$$E_{av}{}^1(d^{n+1}s^1) = E_{av}(d^{n+1}s^1)$$

$$E_{av}{}^1(d^{n+2}s^0) > E_{av}(d^{n+2}s^0) \qquad (23)$$

where the $E_{av}{}^1$ values on the left are calculated by using the frozen orbitals of the $d^{n+1}s^1$ configuration. Both inequalities are due to the fact that the frozen orbitals are optimal for $d^{n+1}s^1$, but not for the other two configurations. As a consequence of eq 23

$$\Delta E_{av}{}^1(d^ns^2 \rightarrow d^{n+1}s^1) < \Delta E_{av}(d^ns^2 \rightarrow d^{n+1}s^1)$$

$$\Delta E_{av}{}^1(d^{n+1}s^1 \rightarrow d^{n+2}s^0) > \Delta E_{av}(d^{n+1}s^1 \rightarrow d^{n+2}s^0) \qquad (24)$$

The sums of the two energy differences in eq 24 are nearly equal[31] in both approximation schemes:

$$\Delta E_{av}{}^1(d^ns^2 \rightarrow d^{n+2}) \simeq \Delta E_{av}(d^ns^2 \rightarrow d^{n+2}) \qquad (25)$$

In summary, in spite of the inequalities in eq 24, the basic similarity between parts A and B of Figure 2 suggests that the frozen-orbital approximation, using $\Delta E_{av}{}^1$, is able to capture some of the essential features of the energy evolution, ΔE_{av}, as a function of N, Z, p, and q.

(31) Equation 25 is in agreement with Slater's transition-state theory[9] suggesting the use of the orbitals of an intermediate configuration in calculating interconfigurational energy differences.

The relevance of this observation becomes clear if we go back to section IV ($N = 1$ systems), where the configurational energy difference $\Delta E_{av}(s \rightarrow d)$ was shown to be quite well approximated by a simple orbital energy difference (eq 14). The close correspondence between parts A and B of Figure 2 now points to an alternative way of approximating ΔE_{av}—through the mediation of $\Delta E_{av}{}^1$—as a simple orbital energy difference. Indeed, from a combination of eq 1 and 20, we find

$$\Delta E_{av}(s \rightarrow d) \simeq \Delta E_{av}{}^1(s \rightarrow d) = \epsilon_{3d}{}^1(d^{p+1}s^{q-1}) - \epsilon_{4s}{}^1(d^p s^q) = \epsilon_{3d,f}{}^1 - \epsilon_{4s,i}{}^1 \quad (26)$$

This equation is formally very similar to eq 14, but now, both orbital energies are based on the frozen orbitals of the $d^{n+1}s^1$ configuration average, and eq 26 is valid for *both* transitions ($d^n s^2 \rightarrow d^{n+1}s^1$ and $d^{n+1}s^1 \rightarrow d^{n+2}s^0$).[32]

Equation 26 can be given a slightly different form, by using eq 20: one obtains for a 4s → 3d transition

$$\epsilon_{3d,f}{}^1 = \epsilon_{3d,i}{}^1 + (3d,3d)^1 - (3d,4s)^1 \quad (27)$$

and therefore at the frozen-orbital level, it is now possible to write down a very simple relationship between the total energy difference associated with a 4s → 3d transition and the orbital energies $\epsilon_{3d,i}{}^1$ and $\epsilon_{4s,i}{}^1$. From a combination of eq 26 and 27, we find

$$\Delta E_{av}(s \rightarrow d) \simeq \Delta E_{av}{}^1(s \rightarrow d) = \Delta E_{av}{}^1(d^p s^q \rightarrow d^{p+1}s^{q-1}) = [\epsilon_{3d,i}{}^1 - \epsilon_{4s,i}{}^1] + [(3d,3d)^1 - (3d,4s)^1] \quad (28)$$

where the first square brackets enclose the energy difference between the two relevant orbitals of the initial configuration, both calculated with the energy parameters corresponding to the $d^{n+1}s^1$ configuration; the second square brackets contain a correction term.

Equation 28 provides a qualitative explanation for the fact that an s → d transition can sometimes be energetically unfavorable, even if the 4s orbital is above 3d. Indeed, the first term in square brackets is negative for all transition metals under consideration (eq 17; Figure 3). Yet, a given (N,Z) transition-metal ion in $d^p s^q$ configuration can lower its energy by dropping an electron from 4s into 3d *only* if the relevant orbital-energy difference is large enough to overcome the second term in square brackets, which is always positive (eq 21). Apparently, $(3d,3d)^1 - (3d,4s)^1$ is the frozen-orbital equivalent of the threshold value, which we had to introduce in our phenomenological description of section V.3. Clearly, if 4s is only slightly above 3d, the larger (dd) repulsion will prevent the electron(s) from leaving 4s and populating 3d.

It is well to stress that eq 26 and 28 are formally identical for the two s → d transitions ($d^n s^2 \rightarrow d^{n+1}s^1$ and $d^{n+1}s^1 \rightarrow d^{n+2}$). This does not mean that both energy differences are predicted to be also numerically identical at the frozen-orbital level. Indeed as shown in eq 20, the ϵ^1 values are configuration dependent, and substitution of eq 20 (together with the corresponding equations for ϵ_{4s}) into eq 28 reveals that

$$\Delta E_{av}{}^1(d^{n+1}s^1 \rightarrow d^{n+2}s^0) = \Delta E_{av}{}^1(d^n s^2 \rightarrow d^{n+1}s^1) + [(3d,3d)^1 - (3d,4s)^1] - [(3d,4s)^1 - (4s,4s)^1] \quad (29)$$

Because of the inequality eq 22, $\Delta E_{av}{}^1$ is always larger for the second s → d transfer than for the first one—in agreement with Figure 2 and eq 16.

The simple rationalization of eq 28 comes into conflict with an earlier attempt of Pilar[16] to relate the relative energy of $d^p s^q$ and $d^{p+1}s^{q-1}$ to an orbital-energy difference. According to Pilar, the additional energy term is not the valence repulsion—as shown in eq 28—but is supposed to be the core–valence repulsion. On the basis of the purely qualitative idea that 4s penetrates the core more than 3d, Pilar assumes that (c,4s) > (c,3d). Table III shows that this assumption is incorrect for $N = 3$; as a matter of fact, it is incorrect for all transition metals and their ions. Although the 4s density is indeed larger than the 3d density in the immediate vicinity of the nucleus, the fact that $r_{3d} < r_{4s}$ leads unambiguously to the conclusion that (c,4s) < (c,3d). It is obvious that the correct treatment, leading to eq 28, is compatible with the latter inequality.[33]

Considering the apparent success of eq 26 and 28, one might wonder whether it would be possible to simplify the problem even further and use one single set of frozen orbitals for M, M^+, and M^{2+} (that is for a given Z and the three different N values).

Attempts along these lines were presented by De Kock and Gray,[17] using a semiempirical approach on the basis of the frozen orbitals of Sc^{2+}. The authors neglected exchange integrals, and at several places they had to make rather crude approximations. Still the idea seems worthwhile to pursue in some detail at the ab initio rather than at the semiempirical level. In order to carry this out quantitatively, we used the orbitals of the intermediate ions M^+ and the intermediate configurations $d^{n+1}s^1$. Let us represent the corresponding frozen orbital parameters by the quantities

$$\omega_{3d}{}^{1+},\ \omega_{4s}{}^{1+},\ (3d,3d)^{1+},\ (4s,4s)^{1+},\ (3d,4s)^{1+} \quad (30)$$

which are just the parameters of eq 19 for M^+. Therefore, for $d^p s^q \rightarrow d^{p+1}s^{q-1}$ in M^+, we have

$$\Delta E_{av}{}^{1+} = \Delta E_{av}{}^1 \quad (31a)$$

and for the corresponding M (with $N + 1$ valence electrons)

$$\Delta E_{av}{}^{1+}(d^{p+1}s^q \rightarrow d^{p+2}s^{q-1}) = \Delta E_{av}{}^{1+} + [(3d,3d)^{1+} - (3d,4s)^{1+}] \quad (31b)$$

while for M^{2+} (being an $N - 1$ electron system)

$$\Delta E_{av}{}^{1+}(d^{p-1}s^q \rightarrow d^p s^{q-1}) = \Delta E_{av}{}^{1+} - [(3d,3d)^{1+} - (3d,4s)^{1+}] \quad (31c)$$

Therefore, the energy required to induce a 4s → 3d transition decreases with increasing atomic charge (at constant Z). This result is correct, but numerically, it fails even semiquantitatively: the $|\Delta E_{av}{}^{1+}|$ values are much too large, both for M^{2+} and for M. Figure 2C shows that the difference with Figure 2A has become rather drastic. In this approximation there is no way to obtain any other ground-state configuration for the neutral atoms but $d^n s^2$; the slope of the d^{n+2} curve for M has the wrong sign, and the largest numerical errors (for both M and M^{2+}) amount to more than 15 eV. We have to conclude that the approximations of eq 31 and Figure 2C have too many drawbacks to be useful as a semiquantitative guide.

VII. Conclusions

The ground configuration of an atom is simply related to the corresponding orbital energies if $N = 1$. In that case, the con-

(32) Actually, when applied to transition metals, the numerical accuracy of eq 26 turns out to be better than that of eq 14—due to a partial cancellation of compensating relaxation effects.

(33) Pilar's argumentation is based on the following general formula (of which eq 10 is a special case), valid for configuration averages:

$$E_{av}(d^p s^q) = \sum_\nu N_\nu \epsilon_\nu - C = \sum_\nu N_\nu \epsilon_\nu - C_v - C_{cv} - C_c$$

where the summation over ν is over all occupied orbitals (core *and* valence; $N_{3d} = p$, $N_{4s} = q$), and where eq 7 has been used. He claims that—since "4s is above 3d"—the quantity $\sum_\nu N_\nu \epsilon_\nu$ (as in eq 10b) has to be larger for $d^p s^q$ than for $d^{p+1}s^{q-1}$. Apparently, this erroneous conclusion is based on a frozen-orbital view (otherwise no simple conclusion of any kind would be possible). Pilar then goes on using the above equation and claiming—incorrectly—that C, more specifically C_{cv}, should be larger for $d^q s^q$. In his view, this would be the only way to reconcile the greater stability of $d^p s^q$ with its (supposedly) larger value of $\sum_\nu N_\nu \epsilon_\nu$. The fallacy of this argument lies in that Pilar *ignores the* ϵ_ν *dependence of p and q*. This has been detailed in eq 20 for 3d, but it is also true for the core orbitals: the orbital energy ϵ_γ of an electron in the frozen-core γ orbital changes if a 4s → 3d transition takes place. It is increased by the amount $(\gamma,3d) - (\gamma,4s)$. Summation over all core orbitals and use of eq 3 yields a total increase in $\sum_\nu N_\nu \epsilon_\nu$ to the amount of (c,3d) − (c,4s). On the other hand, the difference between the C_{cv} terms of the above equation (entering with a minus sign) contributes $-C_{cv}(d^{p+1}s^{q-1}) + C_{cv}(d^p s^q) = -(c,3d) + (c,4s)$, where eq 6 has been used. Therefore, both C_{cv} contributions in ΔE_{av} cancel exactly, and we are left with eq 28, where the explicit dependence on the core–valence repulsion has completely disappeared.

figurational energy difference is given by eq 14, where the two

$$\Delta E_{av}(s \rightarrow d) \simeq \epsilon_{3d,f} - \epsilon_{4s,i} \quad (14)$$

orbital energies are eigenvalues of two different Hartree–Fock Hamiltonians. The validity of this approximation is excellent for the lighter atoms and ions; it correctly predicts the 3d–4s crossover at carbon.

If $N \geq 2$, the conventional $\epsilon(Z)$ curves are no longer appropriate. Indeed, not two, but five different orbital-energy curves are to be considered. Yet, by the use of the frozen orbitals of the intermediate $d^{n+1}s^1$ configuration average, the Hartree–Fock $\Delta E_{av}(s \rightarrow d)$ curves could be reproduced rather satisfactorily. In this case, one finds eq 26, which is formally reminiscent of eq 14.

$$\Delta E_{av}(s \rightarrow d) \simeq \Delta E_{av}{}^1(s \rightarrow d) = \epsilon_{3d,f}{}^1 - \epsilon_{4s,i}{}^1 \quad (26)$$

If *both* orbital energies are calculated in the initial configuration, eq 26 takes the alternative form

$$\Delta E_{av}(s \rightarrow d) \simeq \Delta E_{av}{}^1(s \rightarrow d) = (\epsilon_{3d,i}{}^1 - \epsilon_{4s,i}{}^1) + [(3d,3d)^1 - (3d,4s)^1] \quad (28)$$

where the term in square brackets represents a (positive) threshold value.

In the neutral atoms, $\epsilon_{3d,i}{}^1 - \epsilon_{4s,i}{}^1$ is negative but smaller (in absolute value) than the threshold value (4s above 3d, but only slightly). Therefore, the ground state is characterized by 4s population. Dropping an electron from 4s into 3d would increase both orbital energies with no resulting energy gain. Upon ionization however, the resulting contraction causes a strong increase of the 4s–3d orbital-energy difference, accompanied by a much smaller increase of the valence repulsion so that, for positive ions, it does become favorable to depopulate the 4s orbital. As a consequence, the 4s electrons are "first ionized", although eq 14a shows they were also "first populated".

Acknowledgment. We are indebted to the Belgian Government (Programmatie van het Wetenschapsbeleid) for financial support.

Contribution from the Department of Chemistry, The College of Arts and Sciences, The University of Tokyo, Komaba, Meguro-ku, Tokyo 153, Japan

Relaxation Mechanism of Germanium-73 in Tetrabromogermane and Tetraiodogermane at High Temperature

Toshie Harazono, Katsumi Tanaka, and Yoshito Takeuchi*

Received May 24, 1988

The spin–lattice relaxation time (T_1) and spin–spin relaxation time (T_2) of ^{73}Ge nuclei in $GeBr_4$ and GeI_4 have been measured at various temperatures. It has been shown that T_1 is almost exclusively dominated by the quadrupole relaxation mechanism, while T_2 is dominated by the combination of the scalar coupling and the quadrupole relaxation mechanisms in the high-temperature region.

Introduction

As is always the case with a quadrupole nucleus, the relaxation mechanism of ^{73}Ge nuclei with a spin of $^9/_2$ has not been extensively investigated. For the last few years, however, the relaxation mechanism of symmetric tetrasubstituted alkylgermanes and halogermanes were studied. Thus, the spin–lattice relaxation of ^{73}Ge in tetramethylgermane and tetraethylgermane was found to proceed via the quadrupole relaxation mechanism.[1,2] We also showed that both the spin–lattice and spin–spin relaxations of ^{73}Ge in GeR_4 (R = methyl (Me), ethyl (Et), *n*-propyl (Pr), *n*-butyl (Bu)) were solely through the quadrupole relaxation mechanism.[3]

On the other hand, there remain ambiguities concerning the relaxation mechanism of ^{73}Ge nuclei in tetrahalogermanes. Tarasov et al.[4] showed that the spin–lattice relaxation of ^{73}Ge in $GeBr_4$ was solely via the quadrupole relaxation mechanism while in $GeCl_4$ the relaxation occured mostly via the spin–rotation mechanism above 57 °C and mostly via the quadrupole relaxation mechanism below 57 °C. We found, however, that scalar coupling relaxation was involved in the spin–spin relaxation of ^{73}Ge in $GeCl_4$ and $GeBr_4$.[5,6] We investigated the scalar coupling relaxation of ^{73}Ge in $GeCl_4$ in detail in the temperature range between −50 and +50 °C.[6] In that temperature range, however, the temperature effect on the relaxation time of ^{73}Ge nuclei in $GeBr_4$ and GeI_4 was obscure. We thought that the temperature range investigated was so low for these heavier halogens that we failed to observe the temperature effect.

In the present paper we describe the details of the relaxation of ^{73}Ge in $GeBr_4$ and GeI_4 in the high-temperature region. For this purpose we determined the ^{73}Ge spin–lattice relaxation times (T_1) and spin–spin relaxation times (T_2) of $GeBr_4$ and GeI_4 in the temperature range between 25 and 105 °C.

Table I. Values of T_1(IR) and $T_2(\Delta\nu_{1/2})$ for ^{73}Ge in Tetrahalogermanes

compd	solvent	T_1(IR)/ ms	$T_2(\Delta\nu_{1/2})$/ ms	temp/°C	ref
$GeBr_4$	$CDCl_3$	160	130	30	6
	toluene-d_8	88	81	25	this work
GeI_4	CS_2–C_6D_6 (1:1)	80	80	30	6
	toluene-d_8	51	50	45	this work

Experimental Section

Preparation of Compounds. $GeBr_4$ (bp 82–83 °C (32 mmHg)) and GeI_4 (mp 146 °C) were prepared by the procedures given in the literature.[7] The purity of the compounds was confirmed by the GLC (Shimadzu GC-3BT). $GeBr_4$ (50% v/v) and GeI_4 (0.5 g/1.5 mL) were dissolved in toluene-d_8. The solution was put in an egg-shaped cell and degassed by the freeze–thaw method.

^{73}Ge NMR Spectra. The ^{73}Ge NMR spectra were recorded on a JEOL FX-90Q instrument equipped with the low-frequency insert NM-IT10LF at 3.10 MHz. T_1 was determined by the inversion–recovery method (T_1(IR)), while T_2 was determined by the half-line-width method ($T_2(\Delta\nu_{1/2})$). The error in T_1 and T_2 thus determined was estimated to be about or less than 5%. Other conditions of the measurements have

(1) Sekatsis, I. P.; Liepin'sh, Ê. Ê.; Zitsmane, I. A.; Lukevits, É. *Zh. Obshch. Khim.* **1983**, *53*, 2064.
(2) Takeuchi, Y.; Harazono, T.; Kakimoto, N. *Inorg. Chem.* **1984**, *23*, 3835.
(3) Harazono, T.; Tanaka, K.; Takeuchi, Y. *Inorg. Chem.* **1987**, *26*, 1894.
(4) Tarasov, V. P.; Privalov, V. I.; Drobyshev, S. G.; Buslaev, Yu. A. *Dokl. Akad. Nauk. SSSR.* **1983**, *272*, 1176.
(5) Harazono, T.; Tanaka, K.; Takeuchi, Y.; Kakimoto, N. *Chem. Lett.* **1986**, 1841.
(6) Harazono, T.; Tanaka, K.; Takeuchi, Y.; Fukutomi, H. *Inorg. Chem.* **1987**, *26*, 3851.
(7) Laubengayer, A. W.; Brandt, P. L. *J. Am. Chem. Soc.* **1932**, *54*, 621.

0020-1669/89/1328-1813$01.50/0